IGPP Proposal Number 349

Investigation of Rifting Processes in the Rio Grande Rift Using Data from an Unusually Large Earthquake Swarm

Allan Sanford

Robert Balch

Geophysical Research Center and Geoscience Department
New Mexico Institute of Mining and Technology, Socorro, NM

Hans Hartse

Leigh House

EES-4, Los Alamos National Laboratory, Los Alamos, NM

Grant Period: 10/1/92 - 9/30/93

Reporting Period: 10/1/92 - 9/30/93

Amount Awarded: $20,182

I. Introduction

Bernardo Swarm in the Rio Grande Rift. Because the Rio Grande rift is one of the best seismically instrumented rift zones in the world, studying its seismicity provides an exceptional opportunity to elucidate the active tectonic processes within continental rifts. Our research focuses on the Bernardo swarm which occurred 40 km north of Socorro, New Mexico, in the axial region of the central Rio Grande rift. The swarm commenced on 29 November 1989 and continued for over two years during which time it produced over 40 events with $M_D > 2.0$; four of these in excess of $M_D = 4.3$. This earthquake sequence is the strongest to occur in the rift since 1935 and probably the best recorded instrumentally since seismographs began operating in the rift in the early 1960's.

The Bernardo Swarm and Its Tectonic Setting. Beginning on 29 November 1989, a 15 km^2 region on the axis of the Rio Grande rift near Bernardo, New Mexico (Figure 1), produced the strongest and longest lasting sequence of earthquakes in the rift in 54 years. Although the first event in the sequence was the strongest ($M_D = 4.7$), it was followed two months later by $M_D = 4.6$ and 4.3 shocks and nearly one year later by a $M_D = 4.3$ earthquake. The intensity of the swarm relative to the seismicity throughout the rift becomes apparent when one notes that only six earthquakes with magnitudes greater than 4.0 occurred in the rift in the 30 years prior to the Bernardo Swarm.

The swarm occurred in one of the most intensely studied sections of the rift. The activity is centered approximately 3 km north of VP 150 on COCORP Line 1A [*Brown et al.*, 1980] which transects the rift (Figure 1). The Socorro Magma Body [*Hartse et al.*, 1992], an extensive sill-like feature at mid-crustal depths (approximately 19 km beneath the surface), is the dominant deep feature on Line 1A near the swarm area. The lateral extent of the magma body (Figure 1) has been estimated using reflected phases identified on

DISCLAIMER

microearthquake seismograms [*Rinehart et al.*, 1979], and its internal structure has been studied by *Ake and Sanford* [1988] and *Brocher* [1981]. Maximum surface uplift rates of 2 mm/yr over the magma body have been reported by *Larsen et al.* [1986].

The major structure underlying the epicentral region, revealed by the COCORP line and an industry profile farther to the north, is a shallow northeast-striking, east-dipping and northeast plunging listric fault. Eastward slip along the listric fault has strongly tilted hanging wall Paleozoic and Mesozoic rocks to the west and created a narrow, 4-5 km deep, half-graben along the axis of the rift which has been filled with low-velocity Cenozoic sedimentary rocks.

Data. The swarm was recorded by a permanent, telemetered network of from 8 to 10 stations (Figure 1). Recording was supplemented with temporary stations for periods of days following each event of $M_D \geq 4.0$. Location of hypocenters for swarm events did not depend solely on readings of first-arriving P phases and their associated S phases. Whenever observed, we included reflected phases P_zP, S_zP and S_zS from the mid-crustal magma body in the location process using the joint hypocenter determination program SEISMOS written by *Hartse* [1991]. The use of reflected phases has been shown to reduce focal depth errors of Socorro area earthquakes by a factor of three over the use of direct phases only [*Hartse*, 1991].

II. Progress During the Reporting Period

A. Major Findings

Hypocenters. COCORP Line 1A shows that the epicentral region is immediately above the deep (4-5 km), narrow graben formed by eastward slip along a major listric fault. We initially believed that the low-velocity Phanerozoic rocks in this complex graben would not be a problem in the determination of hypocenters. Previous studies to the south in the Rio Grande rift generally placed hypocenters below 5 km. We assumed that travel through any low-velocity rock could be accounted for with station corrections. Therefore, our first velocity model did not include a low-velocity Phanerozoic layer. Ninety-one percent of the focal depths obtained with this velocity model were between 4.0 and 6.5 km. Thus there was an indication that some of the shallow shocks could have had hypocenters within the hanging wall of the listric fault.

Using the work of *Brocher* [1981] and *de Voogd et al.* [1988] on the shallow velocity structure along COCORP Line 1A, we developed a new velocity model which incorporates a 4.4 km thick Phanerozoic layer above the flattened part of the listric fault with an average velocity of 3.5 km/sec. With this model, we obtained hypocenters for 297 shocks of which 143 had errors in latitude and longitude of ≤ 0.35 km and in depth ≤ 0.5 km. The distribution of epicenters for the 143 shocks meeting these rather stringent error constraints are shown in Figure 2. Most of the epicenters are tightly clustered in a 10 km^2 area and show no obvious linear alignments.

The most informative cross-sections for the events in Figure 2 are A-A′ and E-E′ (Figures 3 and 4). These sections show that the seismogenic zone for this swarm is exceptionally thin, on the order of 1.5 km. They also show that all hypocenters are probably above the flattened part of the listric fault and within the Phanerozoic section. Note in section A-A′ (Figure 3) that the seismogenic zone is dipping to the northeast which is the direction of plunge on the major listric fault underlying the epicentral region.

Fault Mechanisms. We obtained fault mechanisms for 93 earthquakes in the Bernardo swarm which had six or more first motion readings. The computer program we used [*Reasenberg and Oppenheimer*, 1985] ranks the derived fault mechanisms using two criteria which are statistical indicators of the quality of solution. The highest quality solutions are ranked A|A. From the 93 fault-mechanisms, we identified 35 that were A|A solutions and also met the stringent requirements on location errors (Figure 5), that is an error in latitude and longitude ≤ 0.35 km and error in depth ≤ 0.5 km. Two thirds of this group have strike-slip fault-mechanisms with P axes nearly horizontal and tightly clustered from S to SSW (or N to NNE). The remaining third are a mixture of normal and reverse mechanisms, mostly reverse, without any preferred orientations for strike or dip.

Of the less well-constrained fault-mechanisms, the most interesting are those suggesting the possibility of rupture along very low-dipping fault planes. Four solutions of this type of quality A|B occur in the data set and one of these is for an $M_D > 4.0$ earthquake on 1/31/90. The other $M_D > 4.0$ event in our fault-mechanisms data set had a quality A|A and a strike-slip mechanism with a N-S oriented P axis.

B. Summary and Conclusions

Important characteristics of the Bernardo swarm which have been revealed by this research are listed below:

1. All hypocenters appear to be located in the hanging wall of a major listric fault that strikes and plunges northeast.

2. The seismogenic zone for the swarm is only about 1.5 km thick and its sharp base appears to coincide with the flattened part of the listric fault.

3. The seismogenic zone dips to the northeast which is the direction of plunge on the listric fault.

4. On the order of two-thirds of the earthquakes in the swarm have strike-slip fault mechanisms with P axes oriented from S to SSW (or N to NNE). A small group of shocks have fault mechanisms which suggest movement along very low-dipping fault planes could have occurred.

Considering the shallow (< 5 km) depth of the flattened part of the listric fault, the rock beneath that rupture surface must be brittle. The absence of earthquakes in the brittle crust beneath the listric fault suggests that the earthquakes are not directly generated by a regional stress field. On the other hand, the distribution of foci and the observed focal mechanisms suggest that the earthquake sequence may represent the breakup of the hanging wall of the listric fault caused by down-plunge, gravity-driven movement along the fault surface. The down-plunge slippage could be in response to crustal doming south of the epicentral area due to inflation of the mid-crustal magma body over a period of tens of thousands of years [*Sanford et al.*, 1991]. An alternative explanation is that east-west crustal extension may have been greater north of the epicentral region than in the epicentral region. This could have created space for down-plunge movement along the listric fault.

C. Equipment Obtained and Facilities Used

No new equipment has been obtained for this project. Most data analysis has been done using the New Mexico Tech Geophysics Computer Facility.

D. Tangible Results

Papers in Preparation

Sanford, A., R. Balch, J. Lakings, H. Hartse, and L. House. A link between listric faulting and recent seismicity in the central Rio Grande rift of New Mexico, in preparation for submission to Bulletin of the Seismological Society of America.

Abstracts and Presentations

Sanford, A., R. Balch, J. Lakings, H. Hartse, and L. House, A link between listric faulting and recent seismicity in the central Rio Grande rift of New Mexico, abstract submitted to Fall, 1993 AGU Meeting.

E. Intangible Results

The administration of this project has encouraged collaboration between earth scientists at New Mexico Tech and LANL. In February, 1993 Allan Sanford and Robert Balch visited Los Alamos, and Allan Sanford presented a talk on the seismicity of New Mexico. In April, 1993 Hans Hartse visited the New Mexico Tech campus to discuss the ongoing study of the Bernardo swarm. In addition to these exchanges, Hans Hartse has a computer account on the New Mexico Tech Geophysics Sun network. From his office in Los Alamos he remotely logs on to the New Mexico Tech system, where he installs upgraded software, locates earthquakes, and plots results for immediate viewing by the collaborators at New Mexico Tech.

III. Future of the Project

For FY94 we have been funded to expand our study to include an earthquake swarm which occurred near San Acacia, New Mexico, about 15 km south of Bernardo. From our recently gained experience with velocity models in the central rift, we anticipate that the first stage of the San Acacia investigation will be to estimate a new velocity model. With a new velocity model we will be able to locate events and estimate focal mechanisms. Following the detailed study of the San Acacia swarm, we will concentrate our efforts on an interpretation of observed seismicity with respect to rifting processes and the Socorro magma body.

IV. Funds Received

For FY94 we received $20,182, with $15,182 going to New Mexico Tech and $5000 going to LANL (EES-4). Funds at New Mexico Tech support Robert Balch (a doctoral student) and partially support the Sun network at Socorro. Funds at LANL partially support Hans Hartse, a post-doc with EES-4. Our funding has been extended for FY94 at a level of $25,000, with $20,000 going to New Mexico Tech.

V. Los Alamos Facilities Used

Hans Hartse and Leigh House use the EES-4 Sun network for event processing and e-mail/ftp communications with researchers at New Mexico Tech.

VI. References

Ake, J. P., and A. R. Sanford (1988). New evidence for the existence and internal structure of a thin layer of magma at mid-crustal depths near Socorro, New Mexico, Bull. Seismol. Soc. Am., **78**, 1335-1359.

Brocher, T. M. (1981). Geometry and physical properties of the Socorro, New Mexico, magma bodies, J. Geophys. Res., **86**, 9420-9432.

Brown, L. D., C. E. Chapin, A. R. Sanford, S. Kaufman, and J. Oliver (1980). Deep structure of the Rio Grande rift from seismic reflection profiling, J. Geophys. Res., **85**, 4773-4800.

de Voogd, B., L. Serpa, and L. Brown (1988). Crustal extension and magmatic processes: COCORP profiles from Death Valley and the Rio Grande rift, Geol. Soc. Am. Bull., **100**, 1550-1567.

Hartse, H. (1991). Simultaneous hypocenter and velocity model estimation using direct and reflected phases from microearthquakes recorded within the central Rio Grande rift, New Mexico, Ph.D. dissertation, New Mexico Tech, 252 pp.

Hartse, H. E., A. R. Sanford, and J. S. Knapp (1992). Incorporating Socorro Magma Body reflections into the earthquake location process, Bull. Seismol. Soc. Am., **82**, 2511-2532.

Larsen, S., R. Reilinger, and L. Brown (1986). Evidence of ongoing crustal deformation related to magmatic activity near Socorro, New Mexico, J. Geophys. Res., **91**, 6283-6292.

Reasonberg, P., and D. Oppenheimer (1985). FPFIT, FPPLOT, and FPPAGE: FORTRAN computer programs for calculating and displaying earthquake fault-plane solutions, *U.S. Geological Survey Open File Report, 85-739*, 109 pp.

Rinehart, E. J., A. R. Sanford, and R. M. Ward (1979)., Geographic extent and shape of an extensive magma body at mid-crustal depths in the Rio Grande rift near Socorro, New Mexico, in *Rio Grande Rift: Tectonics and Magmatism*, edited by R. E. Riecker, pp. 237-251, AGU, Washington, D. C.

Sanford, A. R., L. H. Jaksha, and D. J. Cash (1991). Seismicity of the Rio Grande rift in New Mexico, in Neotectonics of North America, edited by D. B. Slemmons, E. R. Engdahl, M. D. Zoback and D. D. Blackwell, 229-244, Geol. Soc. Amer. Boulder, Co.

Figure 1. Socorro area of the Rio Grande rift. COCORP lines are labeled as lines 1, 1a, 2, 2a, 3 and 4. Solid outline denotes the mid-crustal magma body as mapped by *Rinehart et al.* [1979]. Triangles and capital letters identify seismograph stations. The Bernardo swarm was centered about 6 km SE of station BDO. (Figure from *Hartse et al.* [1992]).

Figure 2. Epicenters for earthquakes in the Bernardo swarm. The map is restricted to the 143 event that have errors in latitude and longitude of ≤ 0.35 km and in depth ≤ 0.5 km.

Figure 3. Depth profile along AA′ in Figure 2. Events within 0.75 km of line AA′ are projected into the cross-section.

Figure 4. Depth profile along EE′ in Figure 2. Events within 0.75 km of line EE′ are projected into the cross-section.

Figure 5. Fault-plane solutions for 35 earthquakes in the Bernardo swarm. The fault mechanisms shown are grade A|A as defined by *Reasenberg and Oppenheimer* [1985] and are for events that have errors in latitude and longitude $\leq$ 0.35 km and in depth ≤ 0.5 km. Some events have more than one calculated fault-mechanism. These second and third solutions, which are indicated by an asterix after the origin time, are usually comparable in quality to the first solutions.

Figure 1

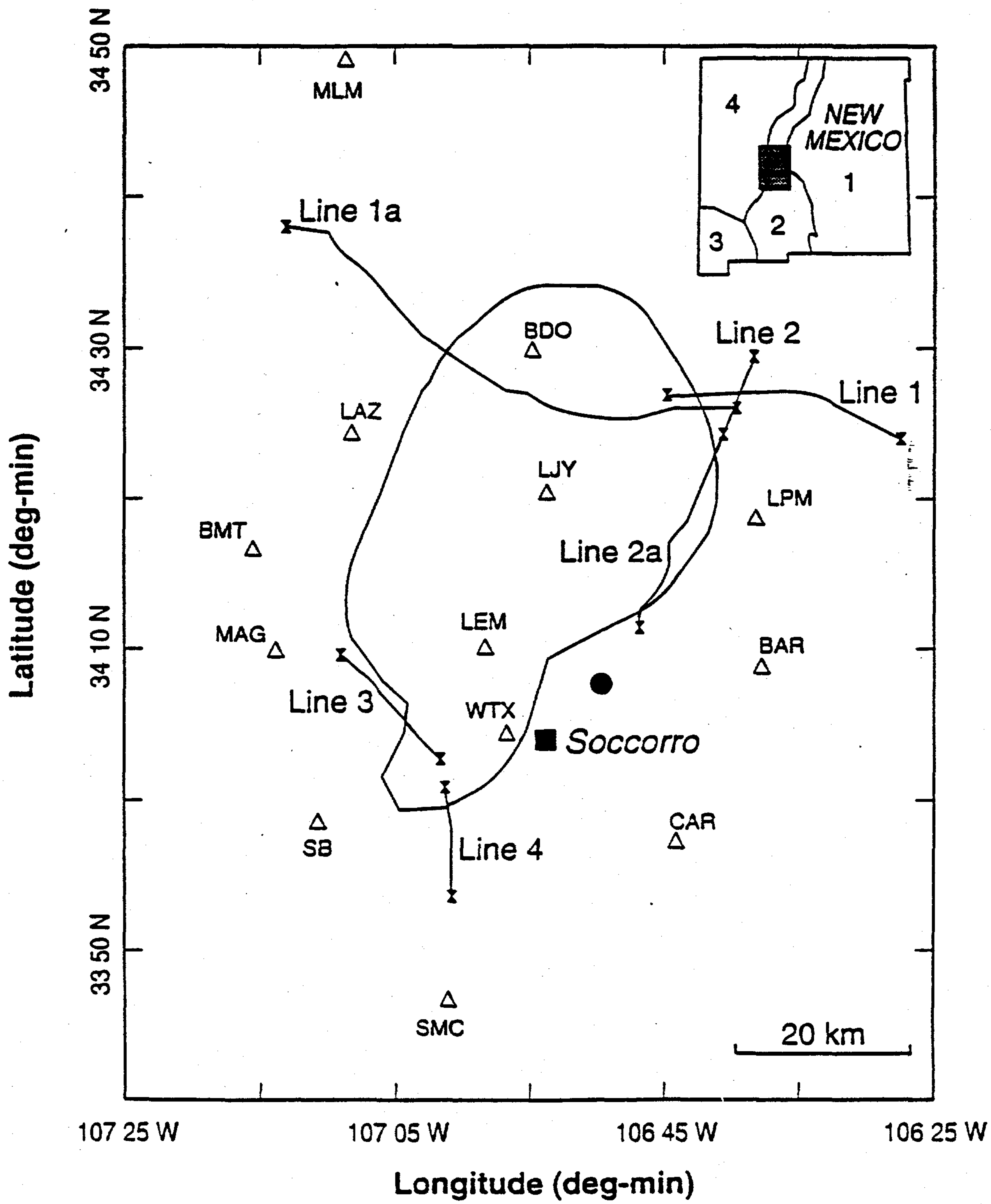

34 50 N
34 30 N
34 10 N
33 50 N
Latitude (deg-min)
MLM
Line 1a
4
NEW MEXICO
1
2
3
BDO
Line 2
Line 1
LAZ
LJY
LPM
BMT
Line 2a
MAG
LEM
BAR
Line 3
WTX
Soccorro
SB
CAR
Line 4
SMC
20 km
107 25 W
107 05 W
106 45 W
106 25 W
Longitude (deg-min)

Bernardo Events - X-sect Proj Dist 0.75 km

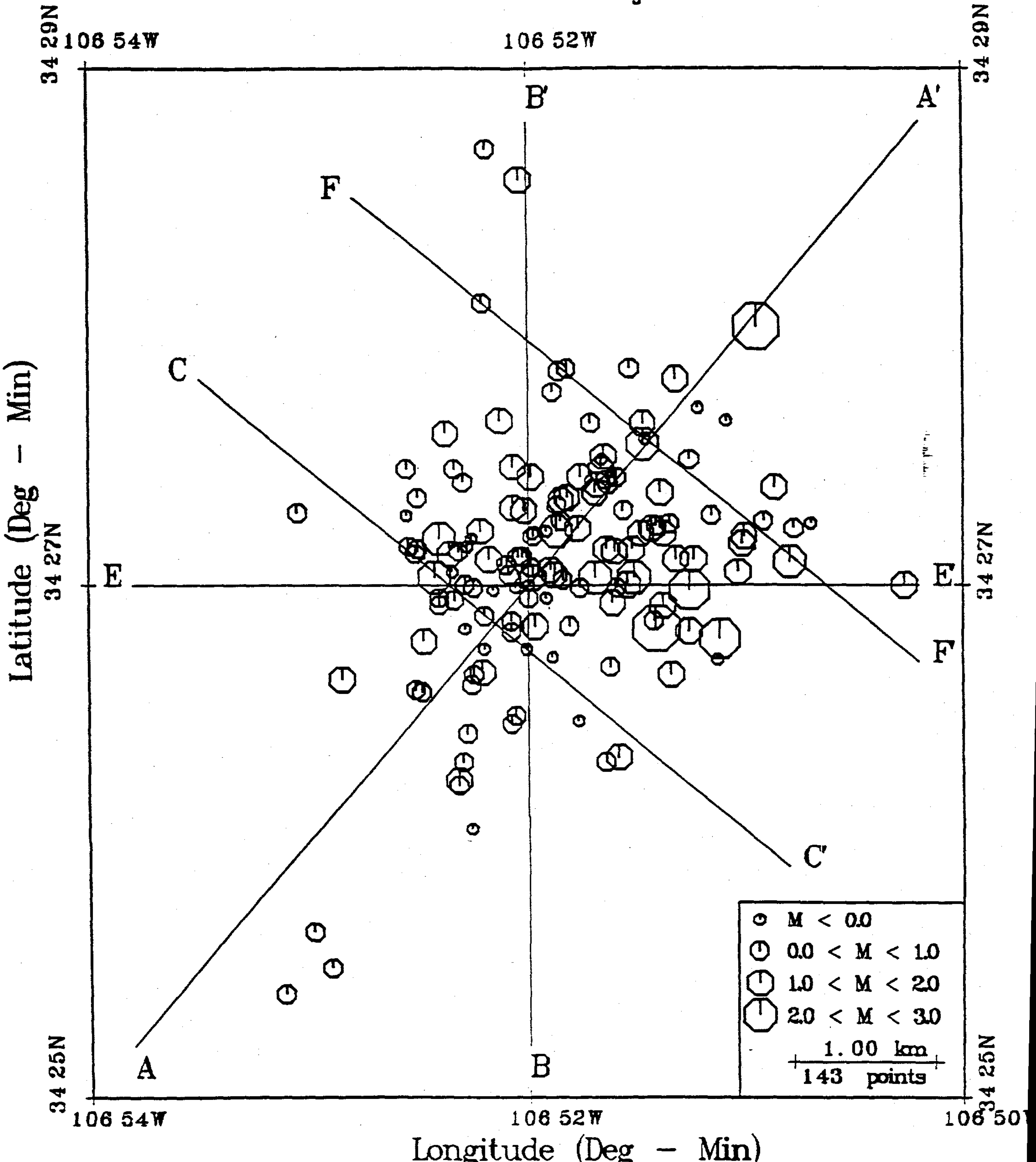

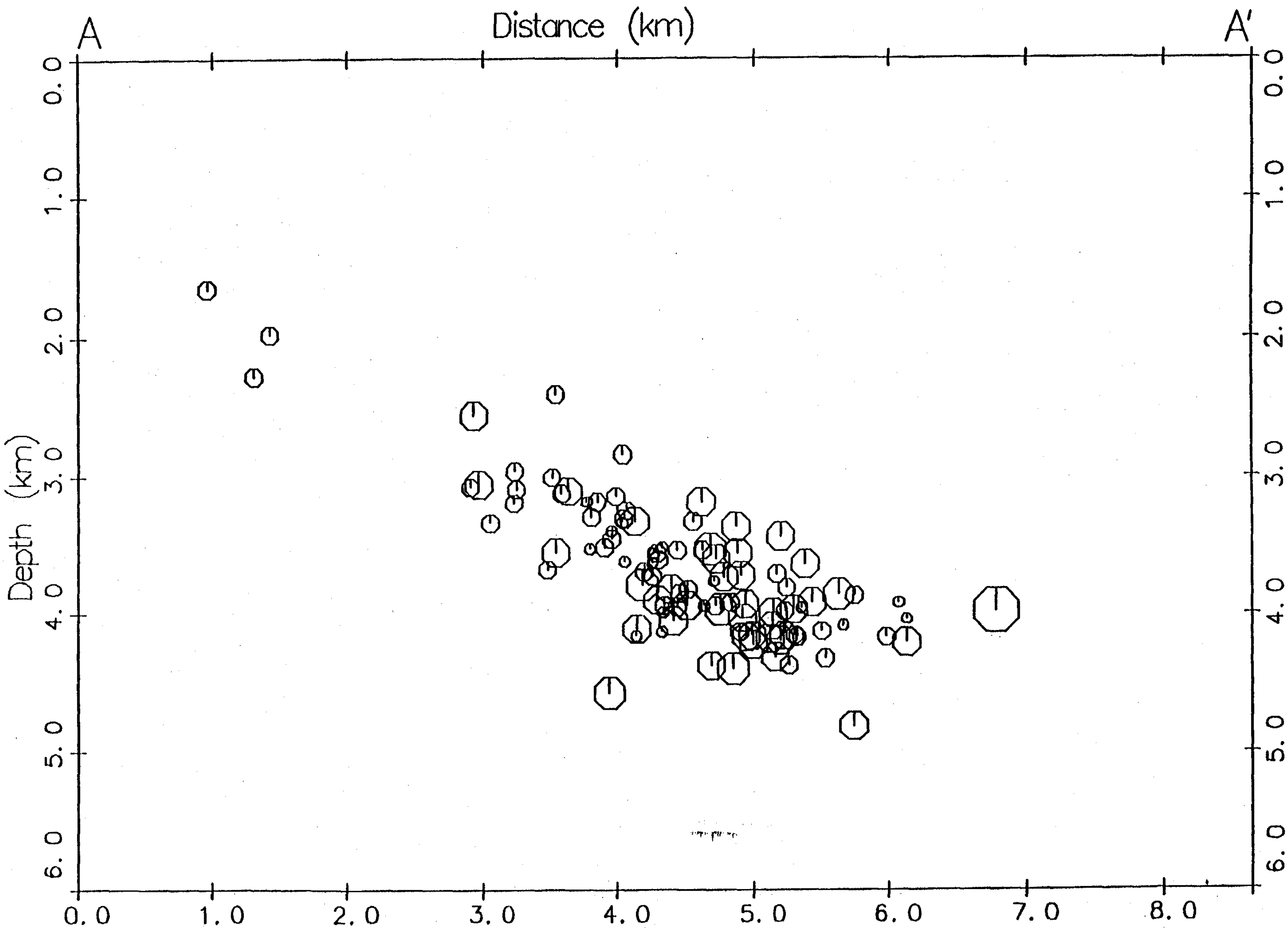
A
A′
Distance (km)
Depth (km)
0.0
1.0
2.0
3.0
4.0
5.0
6.0
7.0
8.0

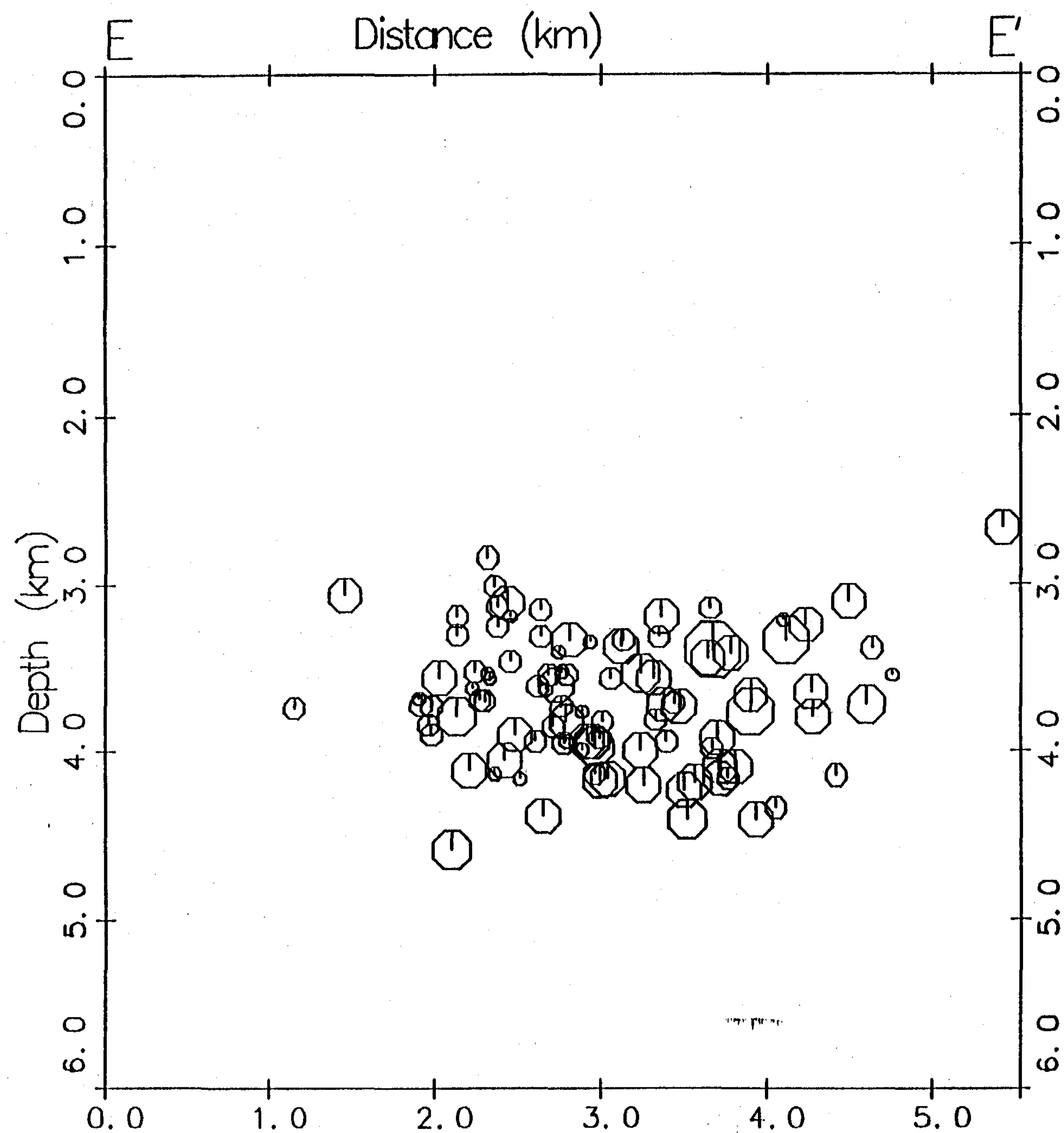
E
Distance (km)
E′
Depth (km)
0.0
1.0
2.0
3.0
4.0
5.0
6.0
0.0
1.0
2.0
3.0
4.0
5.0

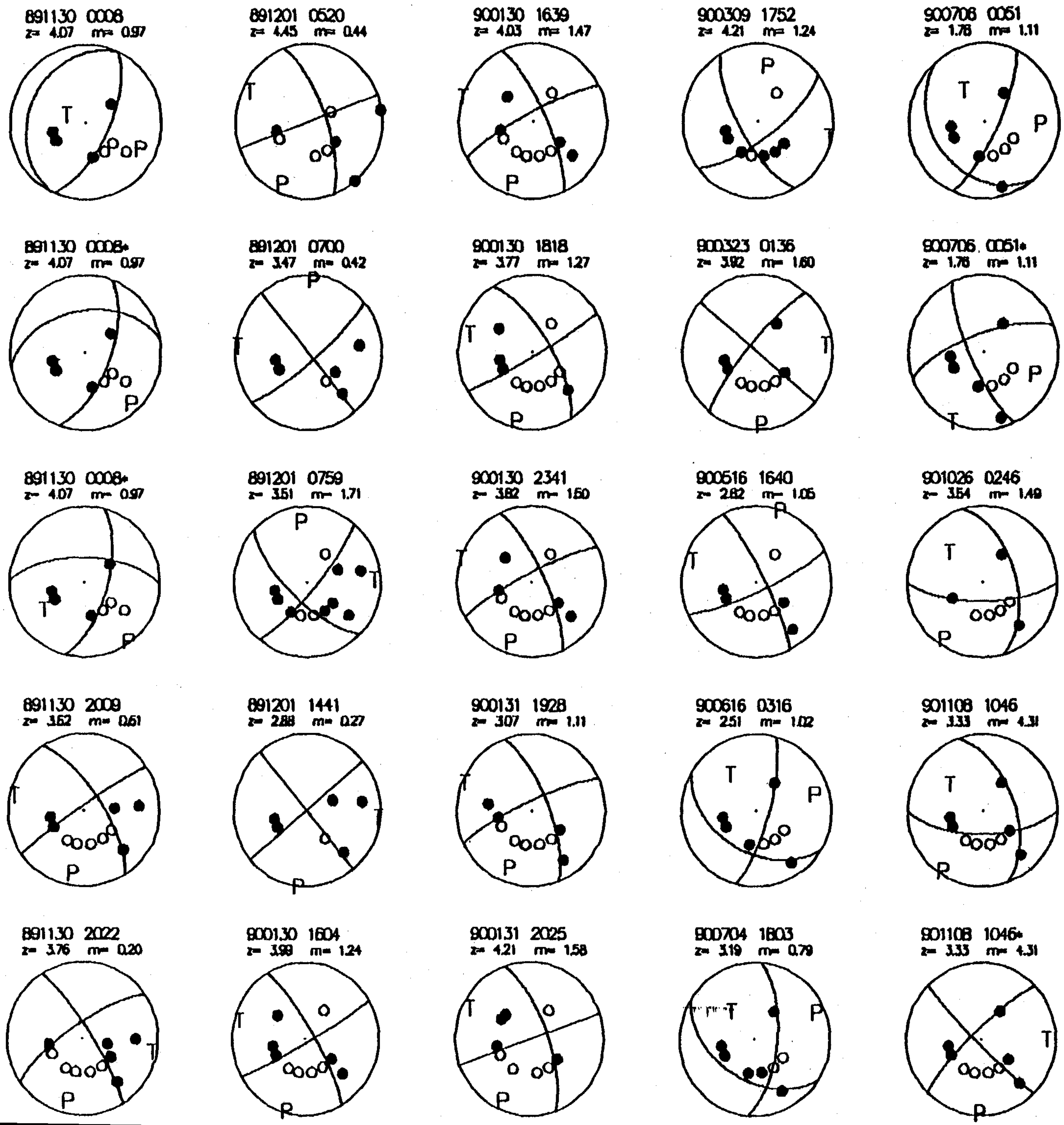

891130 0008
z= 4.07 m= 0.97
891201 0520
z= 4.45 m= 0.44
900130 1639
z= 4.03 m= 1.47
900309 1752
z= 4.21 m= 1.24
900708 0051
z= 1.78 m= 1.11
891130 0008*
z= 4.07 m= 0.97
891201 0700
z= 3.47 m= 0.42
900130 1818
z= 3.77 m= 1.27
900323 0136
z= 3.92 m= 1.60
900706 0051*
z= 1.78 m= 1.11
891130 0008*
z= 4.07 m= 0.97
891201 0759
z= 3.51 m= 1.71
900130 2341
z= 3.82 m= 1.50
900516 1640
z= 2.82 m= 1.05
901026 0246
z= 3.54 m= 1.49
891130 2009
z= 3.62 m= 0.61
891201 1441
z= 2.88 m= 0.27
900131 1928
z= 3.07 m= 1.11
900616 0316
z= 2.51 m= 1.02
901108 1046
z= 3.33 m= 4.31
891130 2022
z= 3.76 m= 0.20
900130 1604
z= 3.98 m= 1.24
900131 2025
z= 4.21 m= 1.58
900704 1803
z= 3.19 m= 0.79
901108 1046*
z= 3.33 m= 4.31

Continued

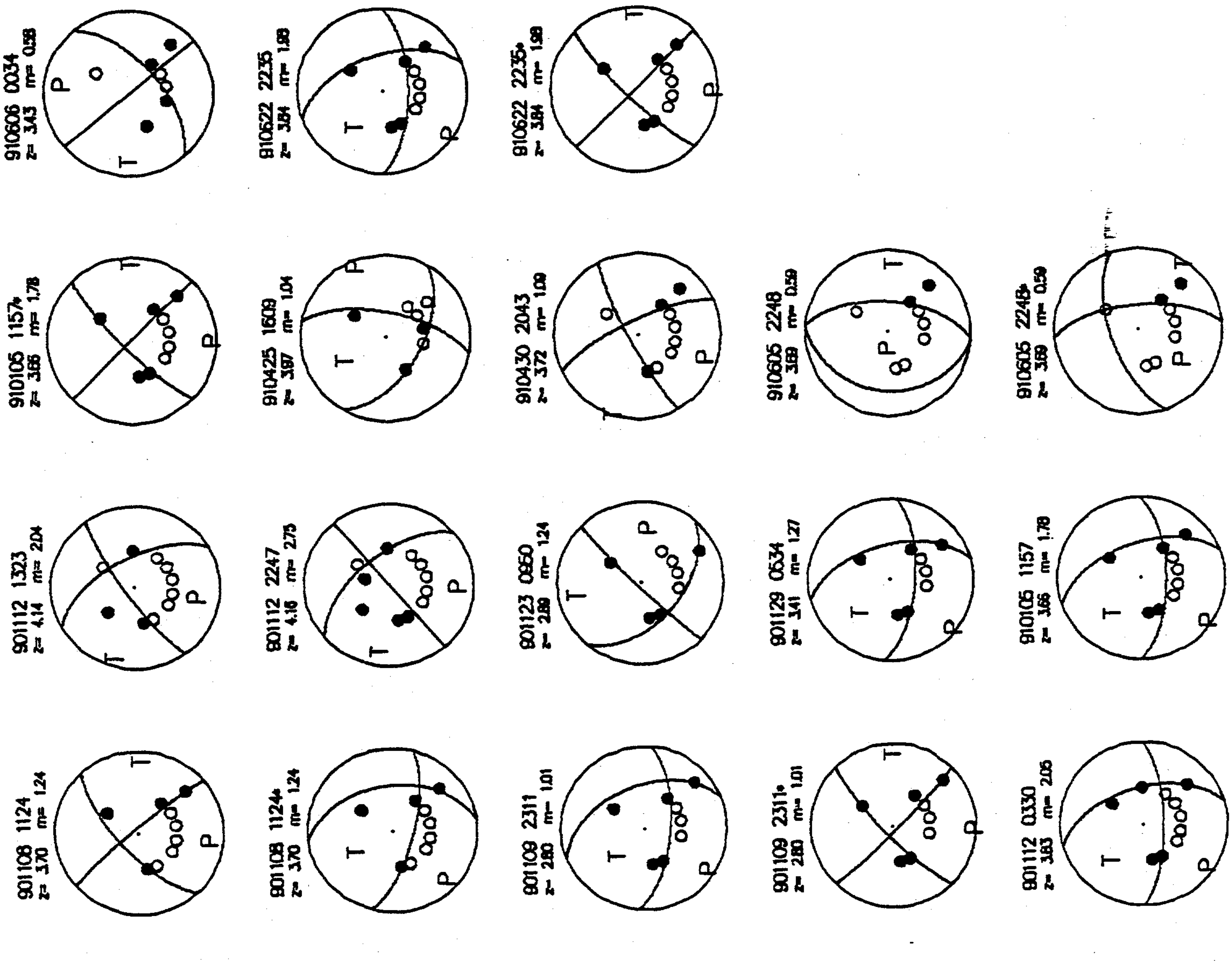

901108 1124 z= 3.70 m= 1.24
901108 1124* z= 3.70 m= 1.24
901109 2311 z= 2.80 m= 1.01
901109 2311* z= 2.80 m= 1.01
901112 0330 z= 3.63 m= 2.05
901112 1323 z= 4.14 m= 2.04
901112 2247 z= 4.16 m= 2.75
901123 0850 z= 2.80 m= 1.24
901129 0534 z= 3.41 m= 1.27
910105 1157 z= 3.66 m= 1.78
910105 1157* z= 3.66 m= 1.78
910425 1609 z= 3.97 m= 1.04
910430 2043 z= 3.72 m= 1.09
910605 2248 z= 3.69 m= 0.59
910605 2248* z= 3.69 m= 0.59
910606 0034 z= 3.43 m= 0.58
910622 2235 z= 3.84 m= 1.93
910622 2235* z= 3.84 m= 1.93